A MOEMS Electrothermal Grating

E. P. Furlani

Integrated Materials and Microstructures Laboratory, Eastman Kodak Company
Rochester, New York 14650-2011, edward.furlani@kodak.com

ABSTRACT

We present a thermoelastically driven MOEMS light modulator in the form of an ElectroThermal Grating (ETG). The ETG consists of an array of equally spaced bilayer microbeams suspended at both ends above a substrate (Fig. 1). The bilayer microbeams have a conductive/reflective top layer that has highly resistive end sections, and a central portion with low resistance, and a nonconductive bottom layer. In an unactivated state, the microbeams are flat and the ETG reflects incident light like a mirror (Fig. 2a). Light modulation occurs when a potential difference is applied across the conductive layers of alternate microbeams. This causes current to flow through the resistive end sections which, in turn, expand due to joule heating. The top sections expand more than the corresponding bottom sections, which have a lower coefficient of thermal expansion. This causes a thermoelastically induced deformation of the heated microbeams downward, toward the substrate. A diffraction pattern is produced when the heated microbeams deform a distance of $\lambda/4$ from their rest position (λ is the wavelength of the incident light) (Fig. 2b). Since the deformation depends on the level of current, an ETG can operate in an analog mode wherein it selectively diffracts a range of wavelengths. In this presentation, we demonstrate the performance of an ETG. We present an analytical design formula for rapid parametric optimization, and demonstrate ETG viability at operating voltages below one volt.

Keywords: MOEMS grating, electrothermal diffraction grating, thermoelastic grating, electrothermal light modulator

1 INTRODUCTION

The ETG is functionally similar to the Grating Light Valve (GLV) which is an electrostatically driven reflective phase grating [1]. Electrostatic actuation has drawbacks in that the activated microbeams have a limited range of motion due to pull-in (1/3 of the gap between the microbeam and the substrate or ground). This limits analog operation where the microbeams need to be deformed to range of depths to modulate a range of wavelengths. On the other hand, if the microbeams are operated in a contact mode (pulled down to the substrate), then only a single wavelength is efficiently diffracted and contact stiction is an issue. Electrostatic actuation has additional disadvantages: it requires relatively high operating voltages (tens of volts) and narrow operating gaps, which can give rise to deleterious squeeze-film effects. Moreover, performance degradation can occur over time due to charge build up in dielectric layers.

The ETG overcomes these limitations. Specifically, thermoelastically actuated microbeams have a full range of motion (no pull-in), which is ideal for analog operation, and their motion is independent of the gap size. Moreover, there is no need for the microbeams to contact the substrate, and therefore, stiction is not an issue. Additionally, the ETG activation voltage is relatively low (less than one volt).

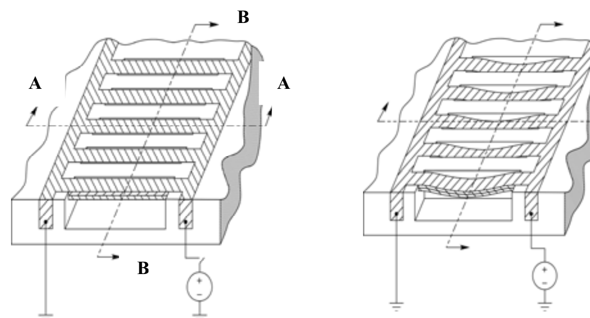

Figure 1: ETG device: (a) unactivated, (b) activated.

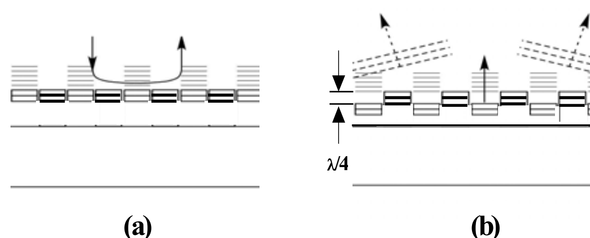

Figure 2: ETG device: (a) unactivated, (b) activated.

The behavior of the ETG is governed by a coupled system of thermal, thermoelastic, and fluidic (gas flow) equations that cannot be solved in closed-form. Nevertheless, analytical models can be developed for evaluating concept viability.

In the following sections we present a one-dimensional quasistatic thermoelastic analysis for predicting ETG performance, and for performing rapid parametric design studies that take into account material properties, dimensions, and operating conditions. We apply the theory to various ETG designs.

2 QUASISTATIC ANALYSIS

The quasistatic thermoelastic deformation of an N-layer microbeam with heated end sections can be predicted to first-order by assuming that a uniform thermal moment M(T) exists along the end sections, labeled by x_1 and x_2 in Fig. 3b. For a given temperature distribution the deformation is governed by the following thermoelastic equation [2]:

$$D_{eq}\frac{d^4 y}{dx^4} = \frac{d^2 M(T,x)}{dx^2}, \tag{1}$$

where y(x) is the vertical deformation along the length of the microbeam (Fig. 3b). T is the temperature distribution along the microbeam, which is assumed to be uniform throughout the thickness of the beam, and M(T,x) is the thermally induced moment. The solution to Eq. (1) for a microbeam, which is rigidly supported ($y = \frac{dy}{dx}$ =0) at either end, is given by

$$y(x) = \sum_{j=1}^{2}(-1)^j\left[-\frac{M_j x^2}{2EI}+\frac{R_j y^3}{6EI}-\frac{M\langle x-x_j\rangle^2}{2EI}\right], \tag{2}$$

where x_j (j=1,2) denotes the edges x_1 and x_2, respectively,

$$M_j = \frac{M(T)\left[2x_j\left(L-x_j\right)-\left(L-x_j\right)^2\right]}{L^2}, \tag{3}$$

$$R_j = \frac{6M(T)\left[2x_j\left(L-x_j\right)\right]}{L^3}, \tag{4}$$

and

$$\langle x-x_j\rangle^2 = \begin{cases} 0 & x < x_j \\ (x-x_j)^2 & x > x_j \end{cases} \tag{5}$$

In these equations

$$M(T) = \frac{C}{B}\sum_{k=1}^{N}\frac{E_k\alpha_k T_k}{1-\nu_k}(h_k-h_{k-1}) - \sum_{k=1}^{N}\frac{E_k\alpha_k T_k}{1-\nu_k}\left(\frac{h_k^{\,2}-h_{k-1}^{\,2}}{2}\right), \tag{6}$$

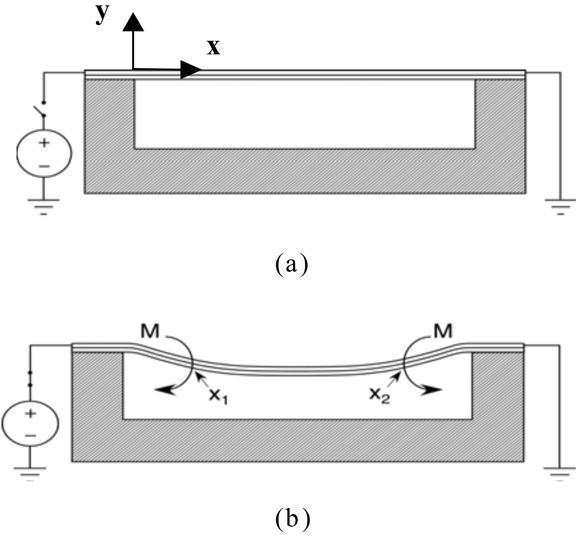

Figure 3: Cross-section of microbeam (A-A in Fig. 1).

and

$$D_{eq} = \frac{BD-C^2}{B}, \tag{7}$$

where

$$B = \sum_{k=1}^{N}\frac{E_k}{1-\nu_k^{\,2}}\left(\frac{h_k-h_{k-1}}{2}\right),\quad C = \sum_{k=1}^{N}\frac{E_k}{1-\nu_k^{\,2}}\left(\frac{h_k^{\,2}-h_{k-1}^{\,2}}{2}\right) \tag{8}$$

$$D = \sum_{k=1}^{N}\frac{E_k}{1-\nu_k^{\,2}}\left(\frac{h_k^{\,2}-h_{k-1}^{\,2}}{2}\right),$$

and E_i, ν_i, and α_i are the Young's modulus, poison ratio, and coefficient of thermal expansion of the i'th layer of the microbeam, h_i is the distance from the surface of the top layer (y=0) to the bottom of the i'th layer, and T_i is the temperature rise in the end sections of the i'th layer ($T_i = \Delta T$ in this analysis).

The solution (2) applies to an N-Layer microbeam with constant cross sectional dimensions, uniform material properties along its length, and negligible heating across its midsection.

The optically active region of an ETG microbeam is the unheated central portion ($x_1 \le x \le x_2$). The average deformation of this section is

$$y_{ave} = \frac{1}{\left(x_2-x_1\right)}\int_{x_1}^{x_2} y(x)\,dx. \tag{9}$$

Therefore, to diffract incident light of wavelength λ, the ETG is designed so that $y_{ave} = \lambda / 4$.

3 DESIGN

There are myriad issues to consider in determining a robust ETG design. Many of these center around the microbeams themselves, their size, spacing, and material properties (structural and thermal). In an ideal microbeam, the resistive end sections should quickly, uniformly, and efficiently heat when activated, and rapidly dissipate their heat to the substrate between activations. Moreover, the end sections should have a high resistance relative to the midsection to maximize thermal deformation. In addition, since the midsection is the optically active region, it should be highly reflective over the entire range of operating wavelengths. Some different microbeam configurations are shown in Fig. 4.

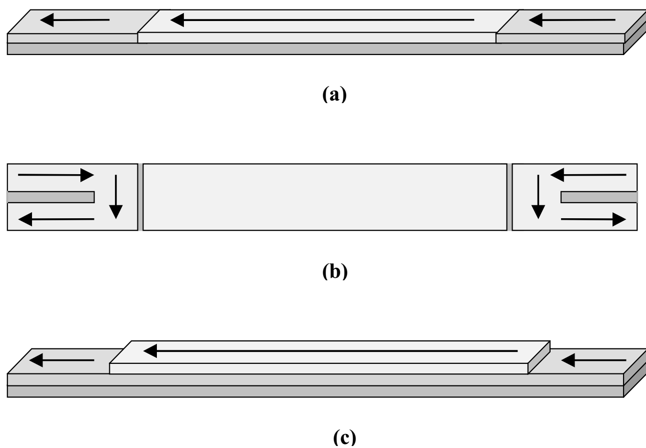

Figure 4: Microbeam configurations showing layer structure and current flow: (a) bilayer structure with low resistance midsection, (b) top view of bilayer structure with isolated midsection (current through end sections only), (c) trilayer structure with low resistance shunt layer.

In Fig. 4 (a) the microbeam has two layers: a nonconductive bottom layer, and a top layer with a conductive/reflective midsection and resistive end sections. For example, the bottom layer could be low stress silicon nitride, and the top layer could have an aluminum midsection with TiAl or TiN end sections. If the structural properties of the top layer vary along its length, then Eq. (2) does not rigorously predict the deformation. Nevertheless, it still can be used to estimate upper and lower bounds for the beam deflection for a given thermal load. It is instructive to determine the temperature rise (ΔT) required to deform this structure to diffract light of wavelength λ = 520 nm. Consider a microbeam that is 3 μm wide and 80 μm long with a 0.25 μm thick TiAl/Al/TiAl top layer and an equally thick, low stress, SiN bottom layer. The end sections are 15 μm long resulting in a 50 μm long optically active midsection. The CFDRC ACE+ multiphysics program was used to compute the deformation of this structure (www.CFDRC.com). The analysis shows that a temperature rise of ΔT= 14°C along (and confined to) the end sections of the beam is sufficient to produce an average deformation of y_{ave} = 130 nm in the optically active region (Fig. 5). The voltage and current required to achieve this ΔT can be crudely estimated using $V = \sqrt{mc\Delta TR / \Delta t}$, where V is the voltage across the microbeam, R is the series resistance of both end sections (midsection ignored), Δt is the duration of the heat pulse (taken to be 1 μs), m is the total mass of both end sections (top and bottom layers), and c is the weighted average of the heat capacities of both end section layers. The voltage, current, and energy required to obtain ΔT = 14°C are estimated to be 294 mV, 5.2 mA, and 1.53 nJ, respectively.

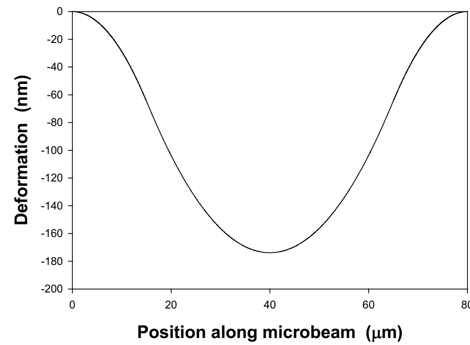

Figure 5: Deformation profile for the microbeam structure of Fig. 4 (a) (ΔT=314°C).

In Fig. 4 (b) the microbeam has uniform material properties except for the gap regions that separate (electrically isolate) the midsection of the top layer from its end sections. During activation, the end sections experience joule heating and the gaps slow the diffusion of heat into the center of the beam. The midsection is coated with a thin (40 nm) layer of aluminum (not shown) so that it will have a high reflectance. The deformation of this structure can be estimated using Eq. (2). Consider a 5 μm wide, 80 μm long microbeam with 0.25 μm thick layers: TiAl on top and low stress SiN on the bottom. Each end section is 15 μm long with a 1 μm wide gap centered width-wise that extends 13 μm along its length starting at the support edge. This gives the end section a U-shaped conductive path. There are 1 μm wide gaps separating the end sections from the midsection, which results in a 48 μm long optically active region. The deformation of this microbeam was predicted using both the analytical model with no gaps, and the

CFDRC numerical program with the gaps included. A comparison of these results is shown in Fig. 6. In this case, ΔT = 19°C yielded y_{ave} = 130 nm for diffracting light at

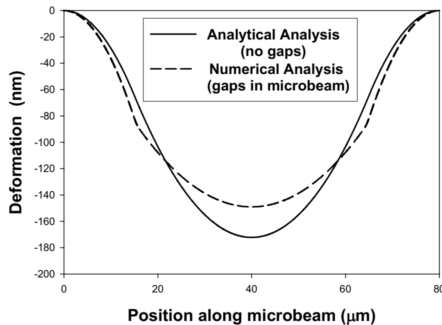

Figure 6: Deformation profile for the microbeam structure of Fig. 4. (b) with 1 μm gaps (ΔT=19°C).

λ = 520 nm. Notice that the gaps produce a flattening of the midsection, which should improve diffraction efficiency relative to the no gap case. This same flattening occurs in electrostatic light modulators when there is only partial electrode coverage [3]. The ΔT of 19° C seems very modest but could have been even lower if the optically active midsection were aluminum (E = 70 GPa) rather than TiAl (E=187 GPa). The voltage required to obtain ΔT = 19°C can be estimated using $V = \sqrt{mc\Delta TR/\Delta t}$ where V is the voltage across one of the U-shaped heater elements, R is its resistance, Δt is the duration of the heat pulse (taken to be 1 μs), m is the mass of the end section (both layers), and c is the weighted average of the heat capacities of both end section layers. For the case studied, the voltage and current required for ΔT = 19°C are 419 mV and 4.13 mA, respectively. The energy required to activate the microbeam is 3.36 nJ. The operating voltage, current, energy and ΔT depend on the length, thickness, and material properties of the microbeam. A parametric analysis of this structure with the TiAl and SiN materials is shown in Fig. 7. The thickness of both layers was set to H, the end sections were fixed at a length of 15 μm, and y_{ave} = 130 nm. The analysis shows that ΔT (and hence energy) decrease with length and thickness as expected.

In Fig. 4 (c) the microbeam has three layers: a bottom support layer, a highly resistive middle layer, and a partial top layer that is reflective and has low resistance. The top layer shunts the current that would otherwise pass through the central portion of the middle layer. Thus, it greatly reduces joule heating in this section. A numerical simulation of this structure was performed in order to determine a viable operating temperature. A 3 μm wide, 80 μm long microbeam was analyzed. The microbeam has three 0.25 μm thick layers: a 50 μm long Al top shunt layer, a TiAl middle layer, and a low stress SiN bottom layer. The end sections are 15 μm long. The analysis showed that ΔT = 25° C was required to produce y_{ave} = 130 nm. This ΔT is higher than in the previous two cases because the microbeam has three layers as compared to two, which makes it less compliant.

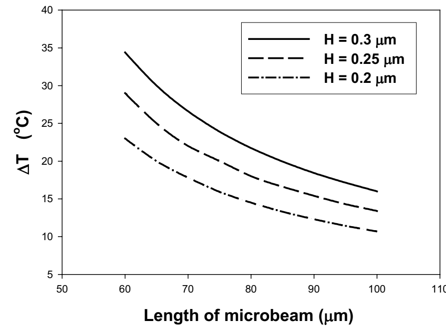

Figure 7: ΔT vs L for the microbeam structure of Fig. 4 (b) (y_{ave} = 130 nm, H = layer thickness).

4 CONCLUSIONS

The ETG shows promise for use in low frequency light modulator applications. Preliminary quasistatic calculations suggest that light modulation can be achieved with modest temperature increases in the active elements (~20°C). The ETG should operate at low voltages (< 1V), and small currents (< 10 mA). Further research is needed to characterize the ETG's frequency response, damping, optical efficiency, and thermal management.

ACKNOWLEDGEMENTS

The author would like to thank J. A. Lebens of Eastman Kodak for valuable discussions on material properties and device fabrication, and Amit Saxena of CFDRC Corp. for his suggestions on structural analysis using the CFDRC program.

REFERENCES

[1] R. B. Apte, "Grating Light Valves for High Resolution Displays," Ph.D. Dissertation, Standard University, 1994..

[2] K. S. Pister and S. B. Dong, "Elastic Bending of Layered Plates," J. Eng. Mech. Div. Proc. Amer. Soc. Civil Eng., 2194, 1959.

[3] E. P. Furlani, E. H. Lee and H Luo, "Analysis of Grating Light Valves with Partial Surface Electrodes," J. Appl. Phys., **83**, 629, 1999.